

**AN EXPERIMENT TO MEASURE THE TEMPERATURE OF THE COSMIC
MICROWAVE BACKGROUND USING
HOME SATELLITE EQUIPMENT**

Daniel R. Elmore

Physics Department

California Polytechnic State University

San Luis Obispo, California 93407

I. INTRODUCTION

I.1. What are Radio Waves?

Radio waves are low-energy electromagnetic waves that travel at the speed of light, or 186,000 miles per second in vacuum (3×10^8 meters per second). In fact, radio waves possess the lowest energy of all other electromagnetic waves with energies less than 10^{-6} eV and wavelengths longer than one meter (and up to several kilometers). The radio part of the spectrum can be divided into frequency (or

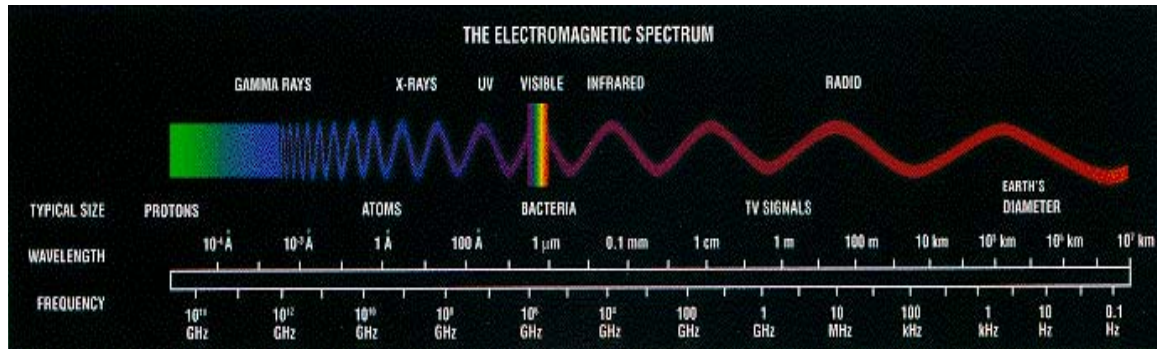


Figure 1 Electromagnetic Spectrum

wavelength) **bands** that help to categorize them for different applications not only in radio astronomy, but for cell phone technology, satellite TV, AM/FM radio, and other areas. The following table lists these radio bands:

Band	Frequency (GHz)	Wavelength (cm)
L	1 – 2	30 – 15
S	2 – 4	15 – 7.5
C	4 – 8	7.5 – 3.75
X	8 – 12	3.75 – 2.5
Ku	12 – 18	2.5 – 1.67
K	18 – 27	1.67 – 1.11
Ka	27 – 40	1.11 – 0.75
V	40 – 75	
W	75 – 110	

Table 1 Radio Bands

Classically, radio waves are generated by disturbances in the motion of electrons. When an electron experiences an acceleration, its electric field, E_θ , in the direction parallel to its motion will be altered [Hey, 11]:

$$(I.1) \quad E_\theta = \frac{-1}{4\pi\epsilon_0} \frac{e\dot{v}(t) \sin \theta}{c^2 r} \exp\left[-i\left(\omega t - \frac{2\pi}{\lambda} r\right)\right], \text{ [Rohlf's, 172]}$$

where ϵ_0 is the permittivity of free space, $8.85 \times 10^{-12} \text{ C}^2 / \text{N}\cdot\text{m}^2$, e is the magnitude of the charge of the electron, $1.6 \times 10^{-19} \text{ C}$, c is the speed of light, $\dot{v}(t)$ is the

acceleration (or deceleration) of the electron, θ is the angle between the direction of r and $\dot{v}(t)$, ω is the oscillation frequency of the electron, t is time, λ is the wavelength of the altered electric field (the radio wave), and r is the distance from the electron to where the radio wave is detected (source to observer). This is not the distance, however, at the time the wave is observed, but the distance at some earlier time, the **retarded time**, when the radiation field was produced. Since radio waves travel with speed c , it takes them a time $t - t_r = \Delta t = \Delta r/c$ to travel Δr [Griffiths, 460].

Objects that emit radio waves can be further narrowed into two categories: **thermal** and **nonthermal** sources. Thermal radiation is the radiation emitted from an object due to its temperature, and the process by which it is radiated is obtained from the quantum mechanical picture of electron transitions within atoms, although the classical picture agrees with this at lower frequencies. A perfect **blackbody** source, a type of thermal source, absorbs all radiation that falls on it. Because it reflects no light, the radiation it emits is due entirely to its temperature. Nonthermal radiation is far more intense than thermal radiation at long wavelengths and has a completely different spectrum, as shown in Figure 2. The main process by which nonthermal radiation is emitted is called **synchrotron emission**. Synchrotron

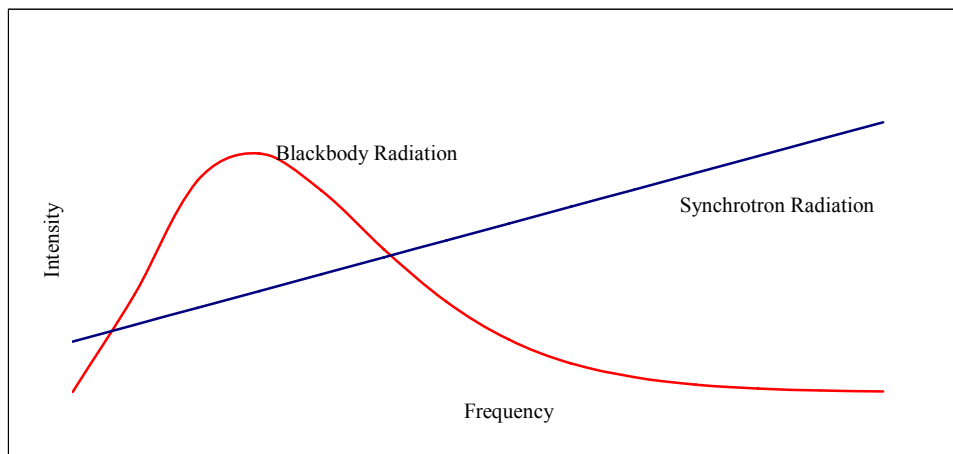


Figure 2 Thermal and Nonthermal Spectra

radiation is due to the acceleration of electrons moving in *circular* motion, which of course is the motion created when electrons (or any charged particle) move through the influence of a magnetic field. This process is responsible for the enormous amount of power that many astronomical objects emit at radio frequencies [Hey, 20].

One type of thermal source that we try to detect in this experiment is the cosmic microwave background (CMB) radiation, an almost completely isotropic source of microwave radiation that permeates the entire universe, giving evidence for the Big Bang theory. The early universe was a very hot and dense plasma composed of quarks and gluons. This plasma was so dense that electrons moved freely, they were not bound to atoms like they are today. Also, the early universe was opaque; the mean free path of photons was very short because there were so many free electrons to scatter them. As the universe expanded, it cooled and reached a certain temperature where electrons could combine with nuclei to form atoms. At this

point, the universe became transparent. As the universe has continued to expand, the photons from that opaque plasma have redshifted and cooled to a temperature of 2.725 K, which is the temperature the CMB is today.

The goal of the experiment described in this paper is to try to get as close as possible to the accepted experimental value of $T_{CMB} = 2.725$ K. Before getting to that point, however, this paper will give the necessary theoretical background for understanding radio telescopes, various antenna parameters, sources of noise, and blackbody radiation. Furthermore, a description of the experimental set-up, the components of the system, and the procedure are given to assist in the reproducibility of this experiment (or related experiments). After the procedure, the data and analysis is shown for two different data runs: the scan of the galactic disk out of the antenna's field of view and the angular scan of the sky.

II. THEORETICAL BACKGROUND

II.1. Antenna Theory

A common type of radio telescope, and the one used in this experiment, is the **parabolic reflector**. As you can see from Figure 3, our dish, and many dishes of this sort, have a wire mesh surface used for directing the radio waves into the feed horn. As long as the holes in the wire mesh are much smaller than the length of the



Figure 3 10 ft. Diameter Parabolic Reflector

radio waves, the holes have no affect on the reflecting power of the telescope.

Once the waves bounce off the wire mesh, they are reflected toward the feed horn, which sits at the **focus** of the dish. In general, the feed horn collects the electromagnetic radiation and passes it to an amplifier and a detector and then to

some type of output measuring device. These devices are connected either by coaxial cables or waveguides. Specifically, the feed horn in this experiment, as with almost all *home satellite equipment*, contains an LNB (Low-Noise Block downconverter). The LNB converts a whole band or *block* of frequencies to a similar band at a lower frequency, called the **intermediate frequency**, IF. This is done by means of a **local oscillator** and a **mixer**; the incoming signal frequency from the feedhorn, ω_S , is combined with a signal frequency from the local oscillator, ω_{LO} , and sent into the mixer, which outputs a beat at the intermediate frequency, $\omega_{IF} = |\omega_S - \omega_{LO}|$ [Tucker, Feldman, 1061]. Thus, the mixer is designed to reproduce the original signal at the desired IF with the smallest amount of loss and the smallest amount of added noise as possible (block diagram in Figure 4). In this experiment, $\omega_{LO} = 5150$ MHz, and $\omega_{IF} = 950 - 1450$ MHz.

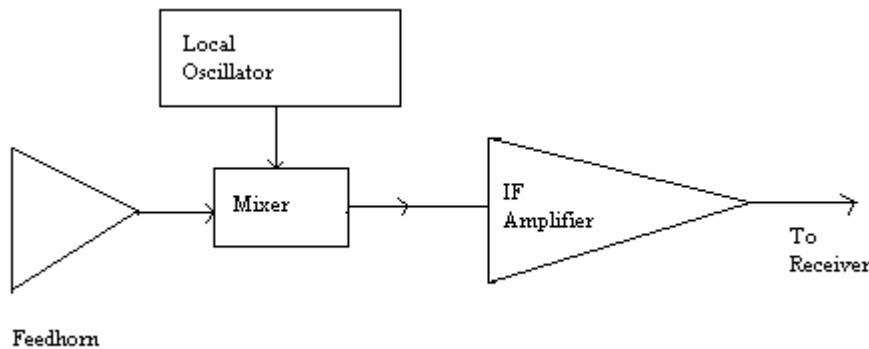


Figure 4 Block Diagram of an LNB

Noise is quantified in two different, yet equivalent, ways depending on what band of frequencies you are considering. C-band LNBs use a quantity known as **noise temperature**, measured in degrees Kelvin (K), to measure the amount of noise in the system. On the other hand, Ku-band LNBs measure noise as a **noise figure**, expressed in decibels (dB) [Long, 3]. The *noise temperature* of the LNB used in this experiment is 57 K (see section **II.2.** below).

II.2. Sources of Noise

Noise is an inherent part of all electrical and electronic systems. As Figure 4 shows, not only does the IF frequency get amplified, but any noise from the mixer and local oscillator will also be sent through the IF amplifier. It is important to understand the sources of noise when working with any type of receiving system, since the noise that is received can be either desirable or undesirable. Thus, we must understand more about the antenna and how radiation is spread across its surface area.

The antenna picks up signals (or noise) from many different sources; even when it is pointed directly upward at the sky, the antenna receives signals from the atmosphere, the ground, the galactic disk, the CMB, and any other types of radio interference such as airplanes and automobiles. These sources all create *noise temperatures* and the total noise temperature of the system is measured in units of

antenna temperature, T_A , and is the sum from all contributions [De Amici, Smoot, *et al.*, 556]:

$$(II.1) \quad T_A = T_{A,\text{atm}} + T_{A,\text{ground}} + T_{A,\text{galaxy}} + T_{A,\text{CMB}}$$

where $T_{A,\text{atm}}$ is the antenna temperature of the atmosphere, $T_{A,\text{ground}}$ is the antenna temperature of the ground, and so on. Furthermore, the antenna temperature for a blackbody at a temperature T covering the antenna aperture is given by [De Amici, Smoot, *et al.*, 556]:

$$(II.2) \quad T_A = \frac{T_v}{e^{T_v/T} - 1}$$

where $T_v = hv / k = 0.226$ K at 4.7 GHz, h is Planck's constant, v is frequency, and k is Boltzmann's constant.

II.3. Antenna Parameters

From the previous section we know that everything that has a temperature emits radiation and thus, introduces noise into our receiving system. But the amount of noise that enters depends on many factors: antenna design, the direction the antenna is pointed, the antenna's **beamwidth**, the **effective area** of the aperture, and the **gain**.

When a radio telescope is aimed directly at a radio source, it gives the maximum signal; as the source moves away, or the telescope moves slightly away from the source, it still receives some of the signal. A good radio telescope will show a signal strength drop to zero very quickly as it moves away from a radio source, which is to say the telescope has a *narrow* beamwidth. An ideal radio telescope gives the most narrow beamwidth with the highest resolving power. By definition, the beamwidth of a radio telescope is the angle between the directions corresponding to half the maximum power (also called the *half power beam width*, HPBW). For circular aperture antennas, the beamwidth θ is given by [Rohlfs, 76]:

$$(II.3) \quad \theta = 58.4^\circ \frac{\lambda}{D}$$

where λ is the wavelength of the incoming radiation and D is the diameter of the aperture. For example, the dish used in this experiment has a diameter of 10 feet, or 3.05 meters, and is used at a wavelength of 6.38 cm (4.7 GHz). So, this system has a beamwidth $\theta = 1.22^\circ$. Figure 5 is a polar plot showing the dependence of direction on the receiver's sensitivity to receive power from the **main lobe**. The main lobe is some part of intercepted signal from some larger power pattern, $P_n(\vartheta, \varphi)$, where ϑ and φ are the spherical coordinates of the power pattern. The *main lobe solid angle*, Ω_M , is given by [Rohlfs, 64]:

$$(II.4) \quad \Omega_M = \iint_{\substack{\text{main} \\ \text{lobe}}} P_n(\vartheta, \varphi) d\Omega$$

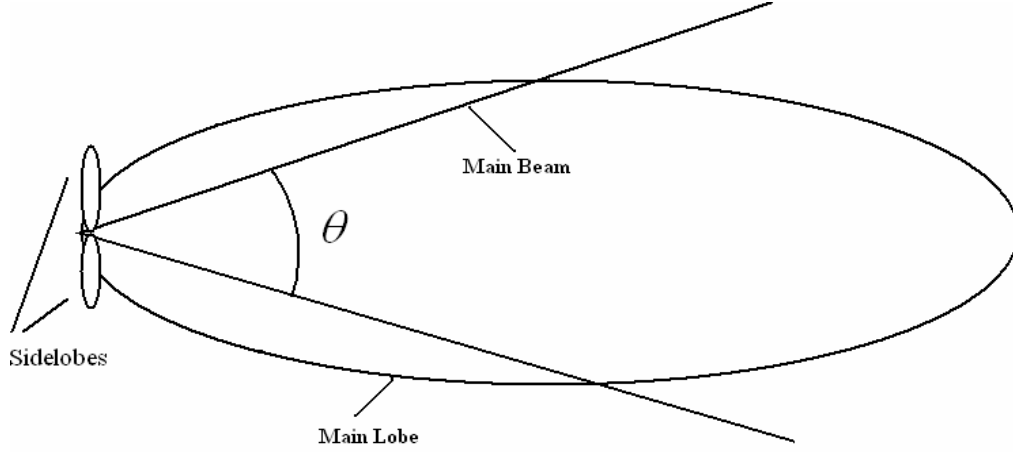


Figure 5 Polar plot of $P_n(\vartheta, \varphi)$ being intercepted by the main beam

measured in steradians, sr. Furthermore, the *beam solid angle*, Ω_A , of the antenna can be defined as:

$$(II.5) \quad \Omega_A = \iint_{4\pi} P_n(\vartheta, \varphi) d\Omega = \int_0^{2\pi} \int_{-\pi/2}^{\pi/2} P_n(\vartheta, \varphi) \sin \vartheta d\vartheta d\varphi$$

From figure 5 we also notice the existence of sidelobes, which are, for receiving purposes, the undesirable parts of the power pattern. How well the power pattern is concentrated in the main beam determines how much information we can know about the radiation source. For example, if we are trying to observe the radiation from a very weak source like the CMB during the daytime, we will get a large amount of noise in the sidelobes due to the very strong signal from the sun. The ground even adds unwanted thermal noise into the sidelobes of a receiving system. However, the function of the parabolic reflector and the feed horn is to produce the highest *efficiency* of the main beam, where the **beam efficiency**, η_M , is defined as [Rohlf, 65]:

$$(II.6) \quad \eta_M = \frac{\Omega_M}{\Omega_A}$$

The **effective area** of the dish, or effective aperture, is the fraction of the dish that collects radio power and sends it to the feed. This is always less than the geometric area of the dish because the feed horn, which sits at the focus, will

collect radiation better from the center than from the edge. The effective area, A_e , can be defined mathematically by [Rohlf, 66]:

$$(II.7) \quad A_e = \frac{P_e}{|\langle \mathbf{S} \rangle|}$$

where $|\langle \mathbf{S} \rangle|$ is the power density of a plane wave being intercepted by the dish and P_e is the amount of power that the feed horn can extract from it. The exact amount of effective area a dish has will vary from system to system; some say a good parabolic reflector has an effective area of 60 percent [Hey, 33], while others contend that most of today's dishes have an effective area of 70 percent [Long, 1]. Thus, the feedhorn attenuates the signal coming from the outer 30 – 40 percent of the dish by as much as 15 dB, acting as a shield for unwanted noise arising from the ground [Long, 1].

The **gain** of an antenna is a measure of how well it can increase the power of a radio signal as compared to some standard. Gain is measured in decibels-isotropic (dBi) or decibel-dipole (dBd), although it is usually expressed just as dB since the standard that we compare this gain to is already implied. For example, the dBi is a measure of the gain relative to some lossless isotropic source. This isotropic source is an imaginary antenna that radiates equally in all directions, and has 0 dBi gain [Ramsey, 1]. The dBd is a measure of the gain relative to a dipole antenna, such as the Hertz dipole, whose gain is known to be $(3/2)\sin^2\theta$.

Gain can be calculated in different ways depending on what specific information is known about the system. One way is to simply take the logarithm of the ratio of output power, P_{out} , to the input power of the signal, P_{in} , and multiply by 10 [Marc, 1]:

$$(II.8) \quad G = 10 \text{Log} \left(\frac{P_{out}}{P_{in}} \right)$$

Another useful formula relates the gain of the antenna to the *effective area* [Hey, 33]:

$$(II.9) \quad G = \frac{4\pi A_e}{\lambda^2}$$

It is interesting to note that in the derivation of equation (II.9), thermodynamic equilibrium between source and receiver is assumed; but since the equation does not contain any thermodynamic quantities, it is always valid [Rohlf, 68]. We can see from (II.9) that a bigger dish gives a bigger gain. Also, the smaller the wavelength of the incoming radiation (i.e. the narrower the *beamwidth*), the higher the gain. Thus, for achieving higher gain and narrower beamwidth, larger radio telescopes are better than smaller ones.

II.4. Atmospheric Attenuation of Radio Waves

There are two regions of the electromagnetic spectrum that are minimally affected by the earth's atmosphere: the visible region and the radio region. What this means is that the atmosphere is *almost* completely transparent to radiation passing through it, within a certain frequency region (Figure 6). For the radio window, this frequency region is from approximately 15 MHz ($\lambda \cong 20$ m) to about

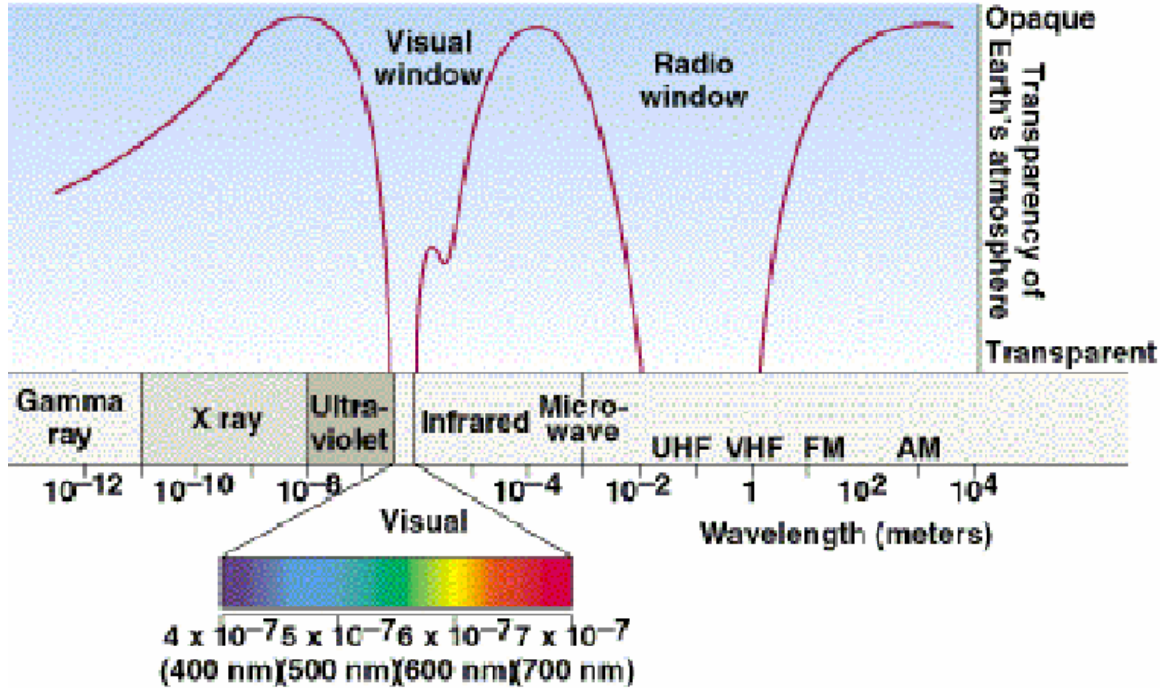


Figure 6 Influence of earth's atmosphere on EM radiation

300 GHz ($\lambda \cong 1$ mm), but these limits can change with geographical location and time [Rohlf, 3]. In this experiment, we are using a frequency of about 4.7 GHz, so we are safely within this range. However, there is a small amount of absorption of radio waves due to moisture caused by water vapor in the atmosphere [Rohlf, 165]. This absorption, although it is small, will decrease the amount of measured power received from a radio source. If $S(z)$ is the radiation flux (power) measured at an angle z from the zenith (straight upward, 0°), and S_0 is the flux that would be obtained outside the atmosphere, then [Rohlf, 165]:

$$(II.10) \quad S(z) = S_0 d^{-X(z)}$$

where d is the attenuation at the zenith for an airmass of h and $X(z)$ is the relative airmass in units of airmass at the zenith. The simplest model, a flat, parallel atmosphere, gives

$$(II.11) \quad X(z) = h \sec z = \frac{h}{\cos z}$$

as shown in Figure 7.

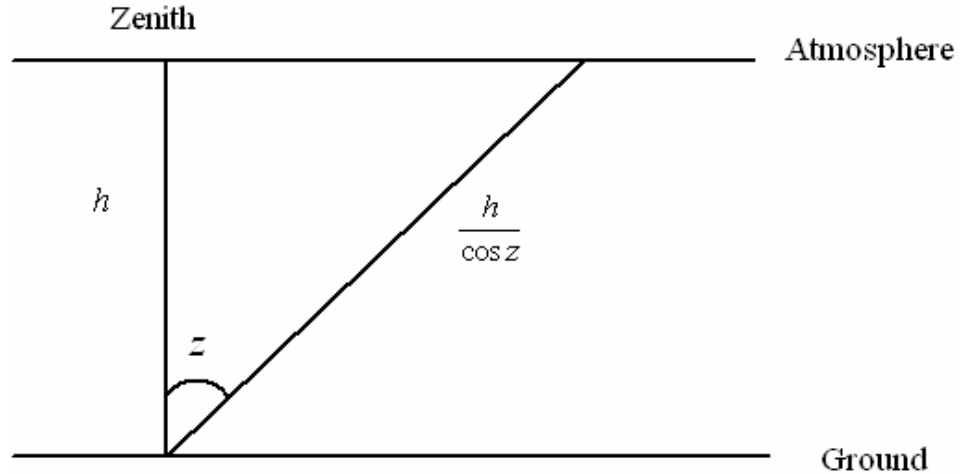


Figure 7 Flat atmospheric model

However, when taking into account the curvature of the earth and the atmosphere, a much more complicated expression arises:

$$(II.12) \quad X(z) = \frac{1}{h} \int_R^{R+h} \frac{\rho(r) / \rho(R)}{\sqrt{1 - \left(\frac{R}{r} \frac{n_o}{n(r)} \right)^2 \sin^2 z}} dr$$

where R is the radius of the earth, $\rho(r)$ is the gas density of the atmosphere at radius r , $\rho(R)$ is the gas density at the surface of the earth, $n(r)$ is the index of refraction of the atmosphere at radius r , and n_o is the index of refraction of the air at the surface of the earth. For our purposes in the analysis section, equation (II.11) is used to show the increase in signal strength from the atmosphere, as you sweep through larger angles. Equation (II.10) and (II.11) together are used to show the decrease in signal strength from a source *outside* of the atmosphere. Because the atmosphere is a weak absorber at this wavelength ($\lambda = 6.38$ cm), it is also a weak emitter, so we have neglected the attenuation due to the atmosphere in this experiment. But it should be noted that the atmosphere can reduce signal strength by about 0.3 % [De Amici, Smoot, 556]. In terms of gain (or loss), the atmosphere can attenuate by about 0.2 dB on a clear day while large rain clouds may attenuate signals by up to 1.5 dB [Rohlf, 165].

II.5. Blackbody Radiation

The blackbody radiation curve in Figure 2 was found theoretically by Max Planck in 1900 using the hypothesis that atomic energy levels are quantized, $E_n = nh\nu$, where n is a nonnegative integer, h is Planck's constant, and ν is the oscillator frequency. The **Planck distribution** is given by:

$$(II.13) \quad B_\nu(T) = \frac{2\pi h\nu^3}{c^2} \frac{1}{e^{h\nu/kT} - 1}$$

where $B_\nu(T)$ is the **brightness** or **intensity** with units $\text{W}\cdot\text{m}^{-2}\cdot\text{Hz}^{-1}\cdot\text{sr}^{-1}$. The Planck law gives the power per area per unit frequency interval per solid angle. In terms of wavelength, the Planck law is

$$(II.14) \quad B_\lambda(T) = \frac{2\pi hc^2}{\lambda^5} \frac{1}{e^{hc/\lambda kT} - 1}$$

If we integrate equation (II.13) over all ν , or (II.14) over all λ , the total power of the blackbody source is obtained:

$$(II.15) \quad B(T) = \sigma T^4$$

$$\sigma = \frac{2\pi^5 k^4}{15c^2 h^3} = 5.67 \times 10^{-8} \text{ W}\cdot\text{m}^{-2}\cdot\text{K}^{-4}$$

This is called the **Stefan-Boltzmann law**, and it shows that the total power per area radiated by an object is proportional to the fourth power of the temperature. If we differentiate equation (II.14), set it equal to zero and solve for λ , we will obtain the wavelength at which the power per area per unit wavelength is maximum; this result is known as **Wien's Law**:

$$(II.16) \quad \lambda_{\max} = \frac{2.898 \times 10^{-3}}{T} \text{ m}\cdot\text{K}$$

For the sun ($T \cong 5900\text{K}$), $\lambda_{\max} = 4.91 \times 10^{-7} \text{ m} = 491 \text{ nm}$. For the CMB ($T \cong 2.7\text{K}$), $\lambda_{\max} = 0.001 \text{ m}$.

In this experiment, however, we are only concerned with a small interval of frequencies (the bandwidth of our LNB). This means that we want to integrate equation (II.13) over some frequency range centered about the incoming signal frequency (4.7 GHz). The bandwidth of our LNB is $1450 \text{ MHz} - 950 \text{ MHz} = 500 \text{ MHz}$ (see section II.1.), so the interval is 250 MHz below 4.7 GHz and 250 MHz above 4.7 GHz. To help simplify the integration, we can approximate the exponential in the denominator of (II.13) as a linear function since we are only looking at a small interval. This is done by taking only the first term in the power series expansion of the denominator:

$$(II.17) \quad e^{hv/kT} - 1 = \frac{hv}{kT} + \frac{(hv/kT)^2}{2!} + \dots \cong \frac{hv}{kT}$$

So, equation (II.13) becomes:

$$(II.18) \quad B_\nu(T) \cong \frac{2\pi k\nu^2}{c^2} T$$

This is the equation we want to integrate over our frequency interval (4.7 GHz – 0.25 GHz, 4.7 GHz + 0.25 GHz) = (4.45 GHz, 4.95 GHz). However, we have to treat the calculation differently for the sun, a **point source**, and the atmosphere and CMB, **extended sources**. For the sun, we only need to integrate over the frequency interval, but for the extended sources, we also need to integrate over the **solid angle** $d\Omega$:

(II.19)

$$B(T)_{\text{point source}} = \int_{4.45\text{GHz}}^{4.95\text{GHz}} \frac{2\pi k\nu^2}{c^2} T d\nu = (3.20 \times 10^{-11} \text{ W} \times \text{m}^{-2} \times \text{K}^{-1} \times \text{sr}^{-1}) T$$

$$B(T)_{\text{extended source}} = \int_{4.45\text{GHz}}^{4.95\text{GHz}} \frac{2\pi k\nu^2}{c^2} T d\nu \int_0^{0.0106} \sin \vartheta d\vartheta \int_0^{2\pi} d\varphi = (3.76 \times 10^{-15} \text{ W} \times \text{m}^2 \times \text{K}^{-1}) T$$

where the upper limit on ϑ -integral is found by taking one-half of the value found using equation (II.3), $\vartheta = 1.22^\circ / 2 = 0.61^\circ = 0.0106$ radians. The solid angle part of the point source equation is taken care of when we calculate power. Power is calculated differently for point sources and extended sources. For an extended source, the power is simply $P = \frac{1}{4\pi} B(T) \cdot \text{Area}$. For a point source, however, the power that we receive depends on its size as well as how far away it is. For the sun, the total power radiated per area (R) is

$$R = B(T) \left(\frac{r_s}{d} \right)^2 = (3.20 \times 10^{-11} \text{ W} \times \text{m}^{-2} \times \text{K}^{-1} \times \text{sr}^{-1}) (5900\text{K}) \left(\frac{6.96 \times 10^8 \text{ m}}{1.50 \times 10^{11} \text{ m}} \right)^2$$

$$= 4.06 \times 10^{-12} \text{ W/m}^2$$

where d is the approximate distance from the earth to the sun and r_s is the radius of the sun. So, the power of the sun is now calculated as $P = R \cdot \text{Area}$.

The diameter of the dish is 10 feet = 3.05 m, so the radius is $r = 1.52$ m. The area, then, is $\text{Area} = \pi \cdot r^2 = 7.26 \text{ m}^2$. Since the *effective area* of the dish is approximately 65%, the total power will be reduced by this amount. Thus, for the CMB, the atmosphere, and the sun, the total effective power intercepted by the antenna is:

$$P_{CMB} = \frac{1}{4\pi} \cdot 0.65 \cdot B(2.725K) \cdot Area = (5.28 \times 10^{-16} \text{ W/m}^2) \cdot (7.26 \text{ m}^2) = \mathbf{3.84 \times 10^{-15} \text{ W}}$$

$$P_{atm} = \frac{1}{4\pi} \cdot 0.65 \cdot B(290K) \cdot Area = (5.63 \times 10^{-14} \text{ W/m}^2) \cdot (7.26 \text{ m}^2) = \mathbf{4.09 \times 10^{-13} \text{ W}}$$

$$P_{sun} = 0.65 \cdot R \cdot Area = (2.64 \times 10^{-12} \text{ W/m}^2) \cdot (7.26 \text{ m}^2) = \mathbf{1.92 \times 10^{-11} \text{ W}}$$

In addition, because equation (II.19) is a relation between intensity and temperature, it follows that:

$$B_{CMB} \propto T_{CMB} \Rightarrow P_{CMB} \propto T_{CMB}$$

$$B_{atm} \propto T_{atm} \Rightarrow P_{atm} \propto T_{atm}$$

Taking the ratio, we get:

$$\frac{P_{CMB}}{P_{atm}} = \frac{T_{CMB}}{T_{atm}}$$

Thus, we obtain a way to calculate the temperature of the CMB based on measurable quantities:

$$(II.20) \quad T_{CMB} = T_{atm} \frac{P_{CMB}}{P_{atm}}$$

III. EXPERIMENTAL SET –UP AND PROCEDURE

III.1. Components of the System

Figure 8 shows the block diagram of the system used in this experiment.

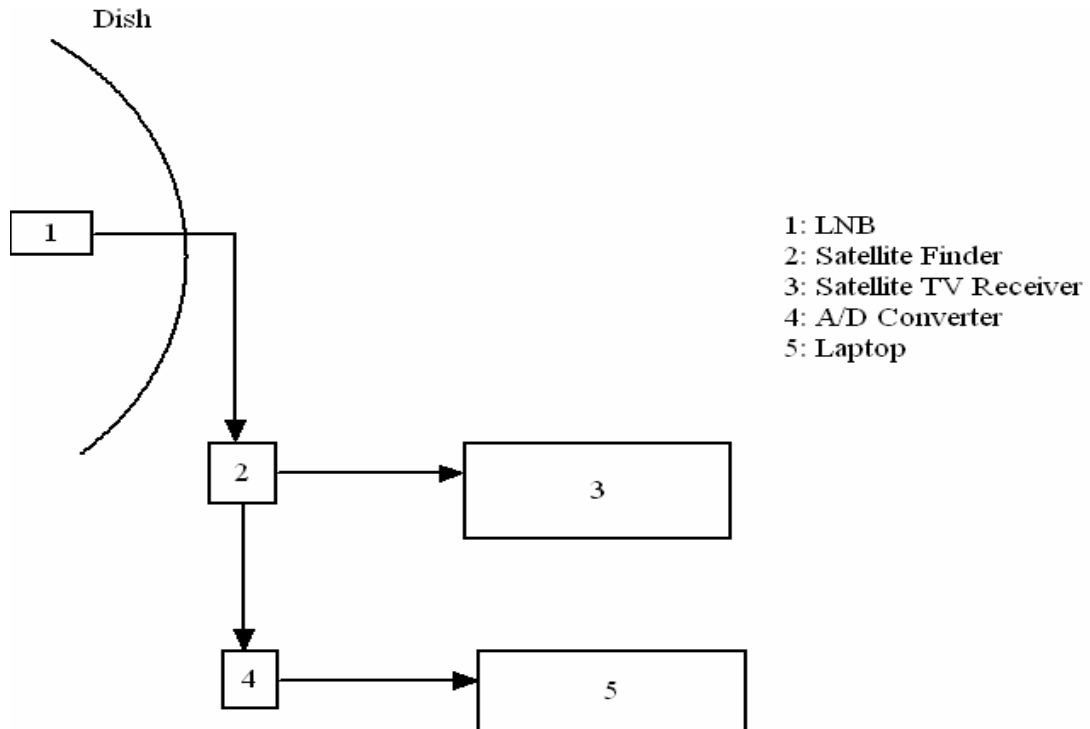


Figure 8 Block diagram of our system arrangement

The **LNB** is a commercial C-band, low-noise block downconverter. It takes an incoming signal at 4.7 GHz, mixes it with a local oscillator frequency of 5.15 GHz, and produces an intermediate frequency between 950 – 1450 MHz, which is then amplified by 30 dB.

The amplified IF signal then travels through coaxial cable to a commercial **satellite finder**, which is the detector used in this experiment. The satellite finder has a signal meter and a sensitivity adjustment on the front panel; its purpose is simply to let you know when your antenna is pointed at a radiating source. Because it has a built-in amplifier, the satellite finder acts as a second stage of amplification. It also has a diode, so that the oscillating radio frequency signal gets converted to a DC output, which is what the signal meter uses to measure the signal strength. The **receiver** has only two functions in this experiment: it is a power supply for the LNB as well as the power and control system for the external motor drive that moves the dish.

The **A/D converter** is a 4-channel, 10-bit data acquisition device that connects directly into a laptop (or PC) serial port. One of the four channels was used as our output, which is displayed in much the same way an oscilloscope is, giving a voltage/division on the vertical axis and time/division on the horizontal axis. This

output is measured from the positive lead of the satellite finder signal meter, while the outside case of the satellite finder serves as the ground. It was necessary to physically open the back of the satellite finder in order to take measurements from the positive lead.

III.2. Procedure

Once all the various components of the system are connected, it is time to **calibrate** it. Calibration is a necessary part of any experiment, since it determines the error associated with a measurement and, if possible, allows you to reduce that error by applying a correction factor to future measurements. Depending on the type of experiment, it may be necessary to calibrate each component of the system, making sure that they are within the specifications set by the manufacturer. However, in this experiment, the individual components were assumed to operate within manufacturer specifications. The calibration in this experiment only involves correlating the power from a known source to the output voltage of that source, the output voltage being obtained from the A/D converter.

One of the set-backs of this system, a set-back which made it very difficult to calibrate, has to do with the *sensitivity adjustment* of the satellite finder. The sensitivity adjustment limits the amount of signal that passes through its amplifier. For a very weak signal, it is best to have the sensitivity at, or near, its maximum level. For a very strong signal, like the sun, the sensitivity should be near its minimum. The problem is that there needs to be *one* sensitivity scale to calibrate measurements on, not multiple scales. This does not mean that our experiment is dead, however.

The experiment *is* dead if we try to make sense of any numerical values without calibrating the system. Yet, if we look at *differences* in numerical values, the data still makes sense. For example, to determine the temperature of the CMB with the system calibrated, we would simply scan the clear sky at different angles starting from the zenith, making sure no other objects are in the antenna's field of view (best to do this in the evening so the radiation from the sun does not enter into the sidelobes). There should be a noticeable increase in voltage as you sweep through larger angles (i.e. $0^\circ \rightarrow 1.1\text{V}$, $10^\circ \rightarrow 2.2\text{V}$, $20^\circ \rightarrow 5.1\text{V}$, ...). These voltages correspond to temperatures (obtained from the calibration curve), and they increase due to the higher amounts of airmass at larger angles (given by equation (II.11)). With the system un-calibrated, we should be able to see this increase in voltage at larger angles. The numerical values of the voltage readings won't make any sense, but the differences in the values should agree with the differences in the values for the calibrated system, giving us a qualitative understanding of how to detect the CMB.

The procedure for detecting the CMB only showed that this system, even set to its maximum sensitivity, is not sensitive enough to detect it. Even with the system un-calibrated, we should have seen the voltage increase, but we didn't (data shown in the next section). Furthermore, on Saturday, March 19, 2005, at about 6:00 pm, the galactic disk was directly overhead. At exactly 6:00 pm that

evening we pointed the dish directly upward and recorded the data as the earth rotated passed it (out of the antenna's field of view). Again, our system was not sensitive enough to detect any change (data in the next section). However, two airplanes did pass through the antenna's field of view during that recording, which is very evident.

IV. DATA AND ANALYSIS

IV.1. Passage of the Galactic Disk

Date: Saturday, March 19, 2005

Time: 6:00 pm

Figure 9 shows a sample of the raw data obtained from the passage of the galactic disk out of the antenna's field of view, where the antenna was pointed at zenith.

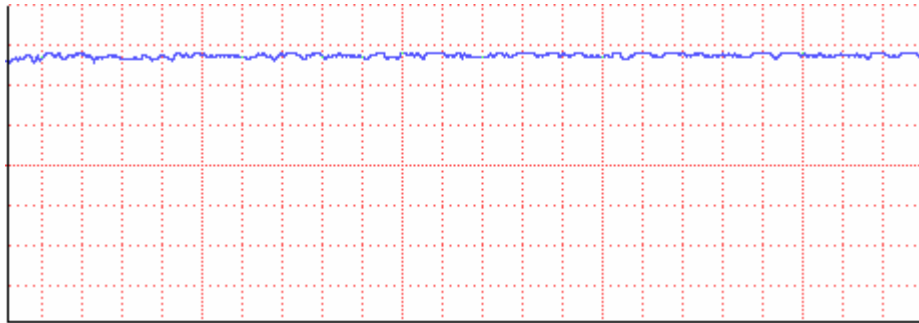


Figure 9 Data acquired from the A/D converter

Figure 9 shows about the first 60 seconds of the recording. Figure 10 is an Excel plot of the entire data run (about 77 minutes). The acquisition rate was 30 samples/second, which should have created a data run lasting 102 minutes, but the data file was full at 77 minutes, causing the recording to stop. However, even in the 77 minute run we should have noticed the signal strength starting to drop as the galactic disk was slowly moving out of the antenna's field of view. Aside from the two airplane interferences that were recorded, there is no noticeable decrease in the signal strength. We do notice a few interesting dips in the signal strength with a magnitude almost as large as the airplane interference. There was some rain that evening, which may have caused some attenuation of the signal from the galaxy. However, we can not be certain of this at this time. Even if the data from the airplane interference is included, it is not enough to change the average value and the standard deviation of the data, which were calculated in Excel. The standard deviation of a set of measurements x_1, \dots, x_N is an estimate of the average uncertainty of those measurements [Taylor, 98], and is given by:

$$(IV.1) \quad \sigma = \sqrt{\frac{1}{N} \sum_{i=1}^N (x_i - \bar{x})^2}$$

where \bar{x} is the mean (or average) value of the data set.

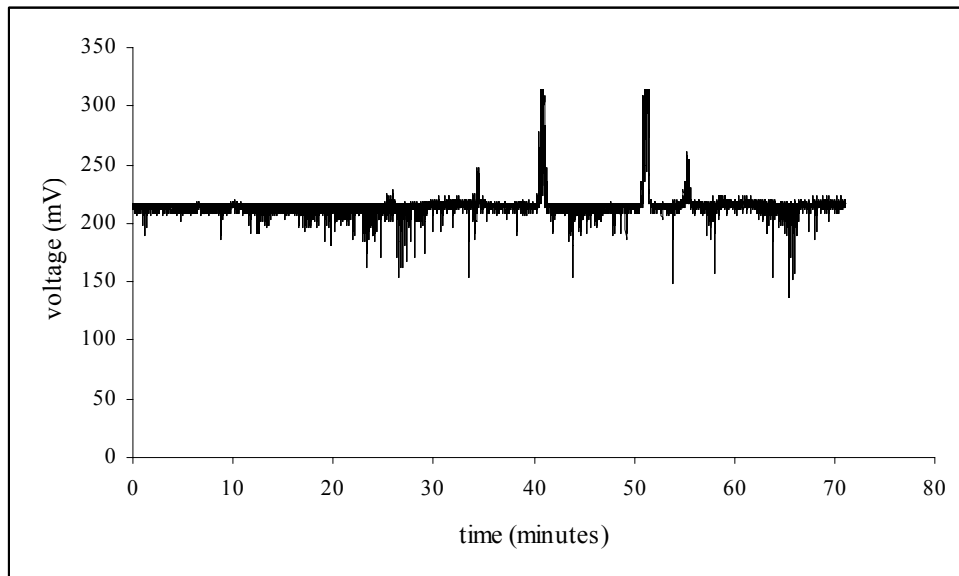


Figure 10 Excel plot from data run of galactic disk

Because there are 34,000 data points from this run, we had Excel calculate the mean and the standard deviation, and we obtained:

$$\bar{V} = 216 \text{ mV}$$

$$\sigma = 10 \text{ mV}$$

Except for the two spikes from the airplanes and the uncertainty of where the dips came from, the baseline voltage of 216 mV did not change, which is an indication that there was probably not enough sensitivity to detect the radio signal from the galaxy.

IV.2. Angular Scan

Date: Saturday, March 19, 2005

Time: 9:30 pm

Figure 11 shows a sample of the data taken from an angular scan of the night sky from different angles, starting from the zenith and proceeding downward (Figure 7).

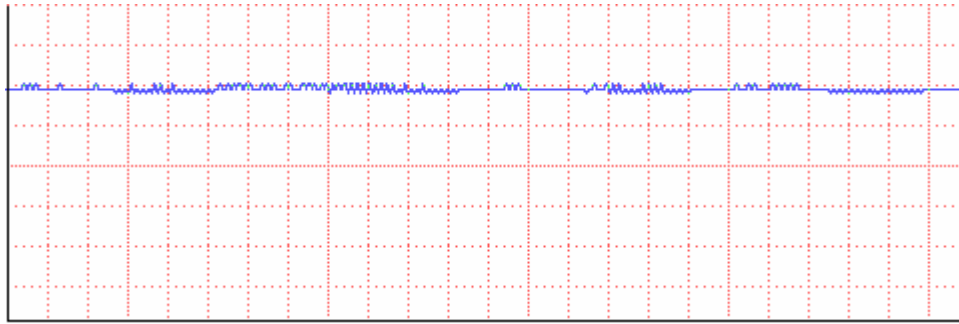


Figure 11 Data from the A/D converter for angular scan

The acquisition rate for this scan was 240 samples/second, which produced a recording lasting about 40 seconds. The angular scan should have shown an increase in signal strength as we moved the antenna through more airmass (larger angles). But as the Excel plot in Figure 12 shows, this does not happen.

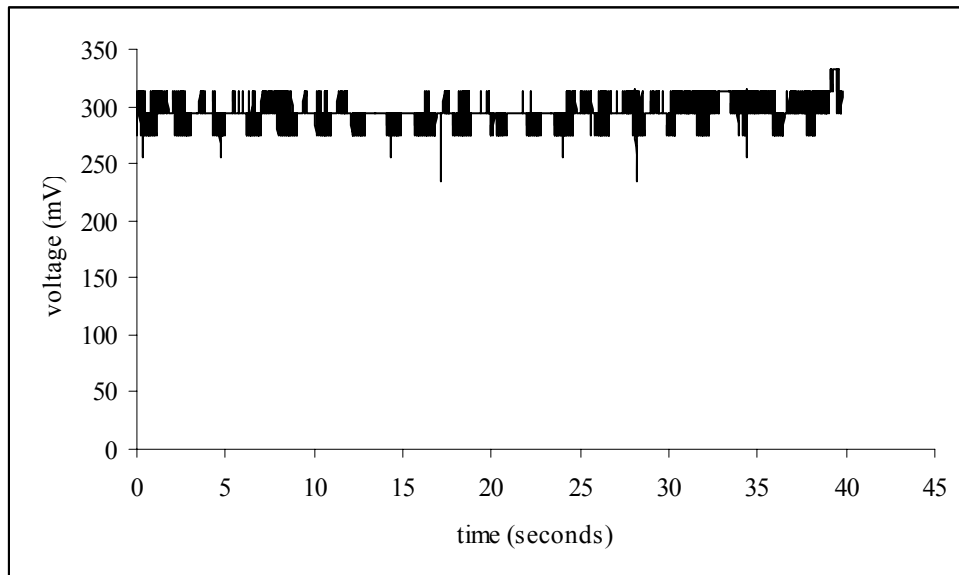


Figure 12 Excel plot from data run of angular scan

This data has a mean and standard deviation of:

$$\bar{V} = 296 \text{ mV}$$

$$\sigma = 12 \text{ mV}$$

where the increase in the baseline voltage to 296 mV was caused by a slight increase in the sensitivity level of the satellite finder. If the system had been calibrated and was sensitive enough to measure the thermal radiation due to thicker airmass, the analysis for determining the CMB would go as follows: Equation (II.11) shows us how the airmass increases with angle. The radiation flux from the atmosphere will increase with increasing angle. However, the radiation flux from the CMB will not vary with angle, it is an isotropic source. Thus, we get a function that is a combination of the CMB and the atmosphere:

$$(IV.2) \quad f(z) = P_{CMB} + P_{atm} \sec z$$

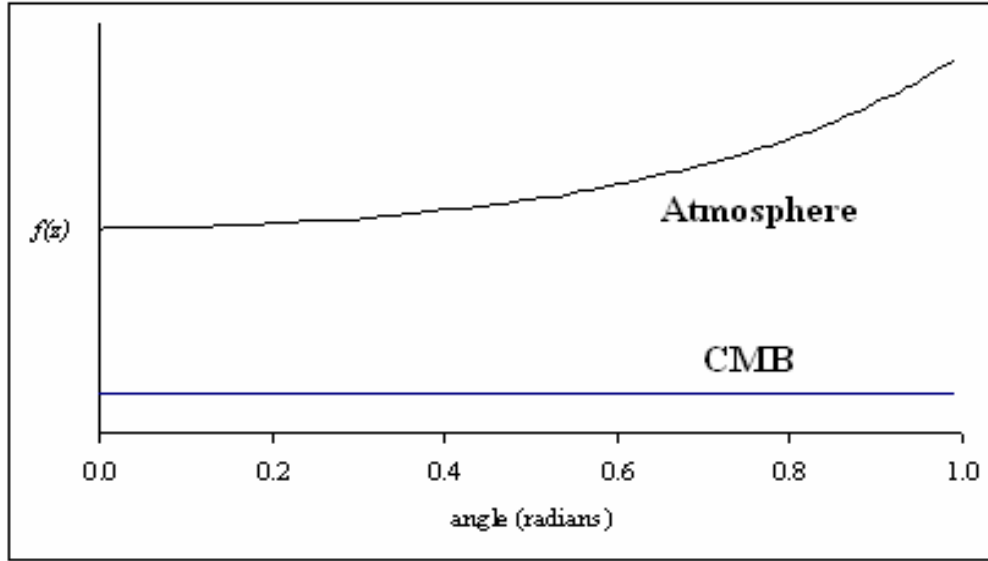


Figure 13 Graphical interpretation of equation (IV.2)

Subtracting the portion due to the atmosphere, we obtain the flux due to the CMB, which is correlated to a temperature, when the system is calibrated. Equation (II.20) in section II.5. is the relevant equation for the temperature of the CMB. It should be noted that the P_{CMB} term in equation (II.20) and (IV.2) will also contain any power due to noise in the system, P_{noise} . Although we have not made a numerical determination of T_{CMB} here (due to the system being un-calibrated), it is likely that we may have only been able to determine the temperature of our system, where $T_{system} = T_{CMB} + T_{noise}$. Yet, since we know that the noise temperature of the LNB is 57 K, this is one source that we could subtract; however, it may not be possible to subtract all the noise in the system, which will add more uncertainty to our numerical figure for T_{CMB} .

V. SUMMARY AND CONCLUSIONS

We have realized the limits of this particular system, but we are still left with some uncertainty as to how limited it actually is. Based on our results, it seems that we obtained no variation in signal strength from the galaxy. However, there is some uncertainty due to the cloud cover and the rain that evening. Yet it seems more likely that our system was just not sensitive enough to detect the galaxy, which means that we would *not* be able to detect the CMB, since at 4.7 GHz the galaxy is roughly one or two orders of magnitude more intense than the CMB [Robinson, 19]. However, more data needs to be taken to determine if this system truly can, or cannot, measure the power from the galactic disk. If it can, then there is still hope for measuring the CMB temperature.

It seems, then, that we leave this experiment with a very important question: how can we improve the sensitivity of this system? One way will be to replace the

satellite finder with an amplifier and detector built specifically for our system. The project will be to build a wide-band IF amplifier (acting as a second source of IF amplification) and a detector module [Capitolo, Lonc, 8]. The output of the amplifier will go to the input of the detector, and the output of the detector will be a positive DC voltage. Building our own detector will give us more control over bandwidth and gain, and will hopefully reduce some of the noise introduced by the second-stage of amplification (the amplifier in the satellite finder is very noisy).

Overall, this experiment has given us a roadmap to pursue future projects and future means of detecting the CMB. With questions and uncertainties come more ideas. The foundations laid here give us something to build on, and the hope of better things to come.

REFERENCES

- Figure 1 taken from: Infrared Astronomy, 2001.
<http://feps.as.arizona.edu/outreach/ira.html>.
- Table 1 of Radio Frequency Bands taken from: Naval Marine TV Antenna Systems, 1997 – 2001.
<http://www.naval.com/radio-bands.htm>.
- Figure 3 taken from: Dave's Web Shop.
<http://www.daveswebshop.com>.
- Ramsey Dennis J. Antenna Systems, 1998.
<http://www.tmeg.com/tutorials/antennas/antennas.htm>.
- Marc. Marc's Technical Page, 2005. <http://www.marcspages.co.uk/tech/antgain.htm>.
- Figure 6 taken from: Radiation and Matter: EM Spectrum: Atmospheric Transparency.
<http://www.ap.stmarys.ca/~ishort/Images/Physics/Radiation/AtmTrans/>.
- Hey JS. 1983. *The Radio Universe*. Great Britain: Pergamon Press.
- Rohlfs Kristen. 1986. *Tools of Radio Astronomy*. Germany: Springer-Verlag.
- Griffiths David J. 1999. *Introduction to Electrodynamics*. New Jersey: Prentice Hall.
- Long Mark. Feedhorns, LNBS and Polarizers, 1997.
<http://www.mlesat.com/Article1.html>.
- De Amici G, Smoot G, Aymon J, Bersanelli M, Kogut A, Levin S, Witebsky C. 1987. Measurement of the Intensity of the Cosmic Background Radiation at 3.7 GHz. *The Astrophysical Journal*, **329**: 556 – 566.
- Taylor John R. 1997. *An Introduction to Error Analysis*. Sausalito, CA: University Science Books.
- Robinson Michael. 1996. *Cosmology*. Oxford: Clarendon Press.
- Capitolo Mario, Lonc William. Classroom Radio Telescope, 1999.
<http://apwww.stmarys.ca/~lonc/radiotel.html>.
- Tucker J.R., Feldman M.J. 1985. Quantum Detection at mm Wavelengths. *Review of Modern Physics* **57**(4): 1060 – 1062.